doi:10.1093/brain/awz090 BRAIN 2019: 142; 1723–1735 | 1723

BRAIN
A JOURNAL OF NEUROLOGY

A multicentre longitudinal study of flortaucipir (^{18}F) in normal ageing, mild cognitive impairment and Alzheimer's disease dementia

Michael J. Pontecorvo,[1] Michael D. Devous Sr,[1] Ian Kennedy,[1] Michael Navitsky,[1] Ming Lu,[1] Nicholas Galante,[1] Stephen Salloway,[2] P. Murali Doraiswamy,[3] Sudeepti Southekal,[1] Anupa K. Arora,[1] Anne McGeehan,[1] Nathaniel C. Lim,[1] Hui Xiong,[1] Stephen P. Truocchio,[1] Abhinay D. Joshi,[1,*] Sergey Shcherbinin,[4] Brian Teske,[4] Adam S. Fleisher[1] and Mark A. Mintun[1,4] for the ^{18}F-AV-1451-A05 investigators

The advent of tau-targeted PET tracers such as flortaucipir (^{18}F) (flortaucipir, also known as ^{18}F-AV-1451 or ^{18}F-T807) have made it possible to investigate the sequence of development of tau in relationship to age, amyloid-β, and to the development of cognitive impairment due to Alzheimer's disease. Here we report a multicentre longitudinal evaluation of the relationships between baseline tau, tau change and cognitive change, using flortaucipir PET imaging. A total of 202 participants 50 years old or older, including 57 cognitively normal subjects, 97 clinically defined mild cognitive impairment and 48 possible or probable Alzheimer's disease dementia patients, received flortaucipir PET scans of 20 min in duration beginning 80 min after intravenous administration of 370 MBq flortaucipir (^{18}F). On separate days, subjects also received florbetapir amyloid PET imaging, and underwent a neuropsychological test battery. Follow-up flortaucipir scans and neuropsychological battery assessments were also performed at 9 and 18 months. Fifty-five amyloid-β+ and 90 amyloid-β− subjects completed the baseline and 18-month study visits and had valid quantifiable flortaucipir scans at both time points. There was a statistically significant increase in the global estimate of cortical tau burden as measured by standardized uptake value ratio (SUVr) from baseline to 18 months in amyloid-β+ but not amyloid-β− subjects (least squared mean change in flortaucipir SUVr : 0.0524 ± 0.0085, $P < 0.0001$ and 0.0007 ± 0.0024 $P = 0.7850$, respectively), and a significant association between magnitude of SUVr increase and baseline tau burden. Voxel-wise evaluations further suggested that the regional pattern of change in flortaucipir PET SUVr over the 18-month study period (i.e. which regions exhibited the greatest change) also varied as a function of baseline global estimate of tau burden. In subjects with lower global SUVr, temporal lobe regions showed the greatest flortaucipir retention, whereas in subjects with higher baseline SUVr, parietal and frontal regions were increasingly affected. Finally, baseline flortaucipir and change in flortaucipir SUVr were both significantly ($P < 0.0001$) associated with changes in cognitive performance. Taken together, these results provide a preliminary characterization of the longitudinal spread of tau in Alzheimer's disease and suggest that the amount and location of tau may have implications both for the spread of tau and the cognitive deterioration that may occur over an 18-month period.

1 Avid Radiopharmaceuticals, Philadelphia, PA, USA
2 Butler Hospital, Providence, RI, USA
3 Duke University Health System, Durham, NC, USA
4 Eli Lilly and Company, Indianapolis IN, USA

*Present address: ImaginAB, Inglewood CA, USA

Received September 12, 2018. Revised January 11, 2019. Accepted February 6, 2019. Advance Access publication April 22, 2019

Correspondence to: Michael J. Pontecorvo
Avid Radiopharmaceuticals, Inc. 3711 Market St. Philadelphia, PA 19104, USA
E-mail: pontecorvo@avidrp.com

Keywords: tau; amyloid; ^{18}F-AV-1451; flortaucipir; PET

Abbreviations: MCI = mild cognitive impairment; MMSE = Mini-Mental State Examination; MUBADA = multi-block barycentric discriminant analysis; NFT = neurofibrillary tangle; SUVr = standardized uptake value ratio

Introduction

Alzheimer's disease is characterized pathologically by extracellular accumulation of aggregated amyloid-β fragments, typically associated with degenerating neurites (amyloid-β neuritic plaques) and by intracellular aggregates of abnormally phosphorylated microtubule-associated tau protein (neurofibrillary tangles, NFTs). Although the density of both amyloid-β neuritic plaques and NFTs at autopsy has been shown to be correlated with ante-mortem cognitive impairment, the degree of association with cognitive impairment has been reported to be greater for NFTs than for neuritic plaques (Cummings *et al.*, 1996; Berg *et al.*, 1998; Nelson *et al.*, 2007, 2012). Moderate-to-frequent neocortical amyloid-β neuritic plaques, consistent with a high level of Alzheimer's disease pathology (Hyman *et al.*, 2012), may be present in 30–50% of clinically normal individuals (Hulette *et al.*, 1998; Price and Morris, 1999; Bennett *et al.*, 2005; Nelson *et al.*, 2007), whereas tau pathology in clinically normal individuals is limited to NFTs in the mesial temporal lobe (entorhinal cortex, adjacent hippocampus, amygdala), and to a lesser extent, inferior temporal regions (Bouras *et al.*, 1994; Price and Morris, 1999; Knopman *et al.*, 2003; Bennett *et al.*, 2005). Widespread neocortical tau deposition, consistent with high Alzheimer's disease tangle pathology, is associated with both significant cognitive impairment and the presence of moderate-to-frequent amyloid-β neuritic plaques (Tomlinson *et al.*, 1970; Knopman *et al.*, 2003; Bennett *et al.*, 2005; Nelson *et al.*, 2007, 2009, 2012). These findings have led to speculation that development of amyloid and tau pathology may begin independently (Nelson *et al.*, 2009; Mungas *et al.*, 2014) but that amyloid-β neuritic plaques may potentiate the spread of NFTs, the more proximal cause of neuronal damage and cognitive impairment in Alzheimer's disease (Nelson *et al.*, 2007).

The advent of PET imaging agents targeting amyloid-β and tau has enabled further exploration of these relationships in living subjects. Three ligands, florbetapir (^{18}F), florbetaben (^{18}F) and flutemetamol (^{18}F) are now approved in major international regions for use in PET imaging of amyloid-β neuritic plaques (Clark *et al.*, 2012; Curtis *et al.*, 2015; Sabri *et al.*, 2015). Subjects clinically diagnosed with Alzheimer's disease dementia or mild cognitive impairment (MCI) likely due to Alzheimer's disease have been shown to have worse cognitive performance (Pike *et al.*, 2007; Johnson *et al.*, 2013), and to deteriorate more rapidly (Doraiswamy *et al.*, 2014; Ma *et al.*, 2014; Baker *et al.*, 2017), if amyloid-positive (amyloid-β+) than if amyloid-negative (amyloid-β−) by PET scan.

More recently, several new tracers targeted at tau NFTs have been reported (Maruyama *et al.*, 2013; Xia *et al.*, 2013; Chien *et al.*, 2014; Okamura *et al.*, 2014; Harada *et al.*, 2016; Hostetler *et al.*, 2016; Declercq *et al.*, 2017; Saint-Aubert *et al.*, 2017; Villemagne *et al.*, 2017; Betthauser *et al.*, 2019; Wong *et al.*, 2018). Although the scope of investigation is still limited for many of these agents, some general themes have begun to emerge, particularly for the most widely distributed of the tau targeted PET tracers, flortaucipir (^{18}F) (flortaucipir, ^{18}F-AV-1451; T807). The pattern of flortaucipir retention on PET imaging parallels the pattern of NFT accumulation reported in autopsy series (Braak *et al.*, 2006; Schwarz *et al.*, 2016). In clinically normal subjects with a negative amyloid PET scan, flortaucipir retention is limited largely to medial temporal lobe. In subjects with positive amyloid PET scans, cross-sectional comparisons suggest increasing and progressive flortaucipir retention in lateral temporal lobe, posterior association cortices and, finally, frontal cortex. This corresponds with increases in estimates of overall tau burden (e.g. cortical composite standardized uptake value ratios, SUVr) across clinical disease stages from clinically normal to MCI to Alzheimer's disease dementia (Brier *et al.*, 2016; Cho *et al.*, 2016*a*; Johnson *et al.*, 2016; Lockhart *et al.*, 2016; Schwarz *et al.*, 2016; Schöll *et al.*, 2016; Pontecorvo *et al.*, 2017*b*). The cortical composite tau PET SUVr also appears to be correlated with cortical amyloid burden (Pontecorvo *et al.*, 2017*b*). But, the regional distribution of the tau tracer PET signal differs from that of amyloid PET tracers, particularly at early disease stages (Brier *et al.*, 2016; Cho *et al.*, 2016*a*, *b*; Harada, 2016; Schöll *et al.*, 2016; Pontecorvo *et al.*, 2017*b*). Cortical composite tau PET SUVr has also been reported to correlate with degree of cognitive impairment (Okamura *et al.*, 2014; Cho *et al.*, 2016*b*; Johnson *et al.*, 2016; Pontecorvo *et al.*, 2017*b*), but the strength of this relationship has varied across studies.

Despite the growing cross-sectional tau PET imaging literature, only one study to date has examined longitudinal change in flortaucipir PET signal (Jack *et al.*, 2018). This study included 59 amyloid-β− cognitively unimpaired, 37 amyloid-β+ cognitively unimpaired and 30 amyloid-β+ cognitively impaired subjects who underwent flortaucipir PET at baseline and 12–15 months. Amyloid-β+ impaired

subjects showed increases (~3% per year) in flortaucipir PET signal (SUVr) across most brain regions, whereas amyloid-β− unimpaired patients showed little change. Amyloid-β+ unimpaired subjects also showed low accumulation of PET signal in most brain regions but significantly more accumulation (~0.5% per year) than amyloid-β− subjects in temporal regions and posterior cingulate.

Further evaluation of the way in which tau accumulation, as assessed by PET imaging, changes over time could be critical to understanding the interaction of amyloid and tau in promoting neurodegeneration and cognitive impairment in Alzheimer's disease (Jack *et al.*, 2016). The present study was therefore designed to provide an exploratory evaluation of the changes in flortaucipir PET tau signal in clinically defined cognitively normal, MCI and Alzheimer's disease dementia subjects, and the association between tau PET signal and 18 month cognitive change in amyloid-β+ subjects, over an 18 month period. Recently, we have reported the cross-sectional baseline PET and cognitive data from this study (Pontecorvo *et al.*, 2017*b*). We now report on the longitudinal change in tau PET imaging and the association of flortaucipir PET and longitudinal cognitive performance.

Materials and methods

Study participants

As described previously (Pontecorvo *et al.*, 2017*b*), 223 subjects were recruited at 25 sites (NCT# 02016560). Sixteen of these subjects were enrolled as a young control group (<50 years of age) with baseline, but not longitudinal, flortaucipir scans. An additional five enrolled subjects were excluded from the present longitudinal analysis—three because their baseline scans were unusable due to technical failure, one because no florbetapir scan was available, and one because no baseline flortaucipir scan was obtained. Thus, a total of 202 subjects (57 clinically defined cognitively normal, 97 MCI subjects, and 48 subjects with clinically-defined possible or probable Alzheimer's disease) were at least 50 years of age, had baseline scans that were quantifiable using the target and reference regions described below, and were eligible for longitudinal analysis. Of these, 33 subjects discontinued before 9 months and an additional 21 discontinued between 9 and 18 months. One subject was excluded from the 9-month analysis (but not 18 months) and three subjects were excluded from the 18-month analysis due to scan technical issues. Thus, 168 subjects completed the 9-month visit and 145 subjects completed the 18-month visit with valid scan and cognitive data (Supplementary Fig. 2 and Supplementary Table 5).

Diagnostic criteria

Subjects were classified as cognitively normal if they had no evidence of cognitive impairment by history or examination and had a screening visit Mini-Mental State Examination (MMSE) > 29. MCI subjects had a diagnosis consistent with National Institute of Aging (NIA)-Alzheimer's Association clinical criteria (MCI-Alzheimer's disease; Albert *et al.*, 2011), were ⩾ 50 years of age and had an MMSE > 24. Subjects in the clinically diagnosed Alzheimer's disease/Alzheimer's disease dementia group were ⩾ 50 years of age, met NIA-Alzheimer's Association core clinical criteria for possible or probable Alzheimer's disease (McKhann *et al.*, 2011) and had an MMSE > 10. Subjects were excluded from participation if they were females of childbearing potential not using adequate contraception, had a history of stroke, current clinically significant cerebrovascular disease, drug or alcohol abuse or dependence, or if they were participating in a trial with other experimental drugs.

Ethics committee

This protocol was approved by the relevant institutional review boards and all subjects or authorized representatives signed informed consent prior to conduct of study procedures. This trial was conducted in compliance with the Declaration of Helsinki and the International Conference on Harmonization guideline on good clinical practice (World Medical Association, 1997).

Study assessments

At baseline, all subjects underwent a clinical diagnostic interview, and a cognitive/functional test battery including MMSE, Alzheimer's Disease Assessment Scale 11-item cognitive subscale (ADAS-Cog$_{11}$), and the Pfeffer Functional Activities Questionnaire (FAQ). An MRI scan performed at screening or within 6 months prior to enrolment ruled out significant CNS lesions and included a 3D T$_1$-weighted sequence that was used for processing the PET images. Additionally, all subjects underwent a florbetapir amyloid PET scan. Flortaucipir PET scans, MRI, and cognitive assessments were repeated at the follow-up visits at 9 ± 2 and 18 ± 2 months. Vital signs, laboratory values and ECG were obtained prior to and after each flortaucipir PET scan, and adverse events were monitored for 48 h post-scan.

Imaging acquisition and analysis

For flortaucipir PET imaging, subjects received an intravenous infusion of ~370 MBq (10 mCi) of flortaucipir (^{18}F), followed ~80 min post-dose by a continuous 20-min brain scan, acquired as four 5-min frames. For florbetapir PET imaging, subjects received an intravenous infusion of ~370 MBq (10 mCi) florbetapir (^{18}F), followed 50 min later by a 10-min brain PET scan acquired as two 5-min frames. All PET data were reconstructed using scanner-specific protocols with the following parameter selections: iterative reconstruction algorithm (FORE, OSEM or RAMLA), 3–6 iterations, 16–33 subsets, 2.0–2.67 mm × 2.0–2.67 mm × 2.0–4.25 mm voxel size. Post-reconstruction Gaussian filters of 3–5 mm were applied (except for Philips scanners where the 'Normal' or 'Sharp' relaxation parameter setting was used). Detector response modelling was not used. Time of flight reconstruction was used at one site.

Florbetapir PET images were visually interpreted as either amyloid-β+ or amyloid-β− by two experienced readers (A.K.A. and M.D.D.) with access to quantitative information (VisQ read, Pontecorvo *et al.*, 2017*a*).

For the analysis of flortaucipir PET data, the 5-min PET images were motion corrected, as well as corrected for time of acquisition to be equivalent to an 80 min post-injection acquisition time (see below), then summed into a single image. The summed image was then co-registered to the subject's T_1-weighted MRI image. The 9- and 18-month PET images were similarly motion and time corrected and summed, then aligned first to the baseline PET image and then to the corresponding MRI image using the same co-registration parameters as the baseline PET scan. The unified segmentation and normalization algorithm in SPM8 was used to transform the T_1 MRI images to MNI atlas space while simultaneously segmenting them into probabilistic tissue maps corresponding to grey matter, white matter, and CSF. The MRI-to-atlas transformation matrix was then used for spatial normalization of the co-registered flortaucipir PET data (Fonov *et al.*, 2011).

Previous studies (Shcherbinin *et al.*, 2016) have suggested that flortaucipir SUVr values may not reach a stable plateau, but may continue to increase throughout the potential imaging window (i.e. up to 150 min post-injection). Consequently, differences in the delay from injection to scan acquisition times across the baseline, 9- and 18-month scans could result in systematic differences in SUVr, with longer delay times leading to higher SUVr, particularly in patients with higher tau burden. Correction factors to address this concern are determined as follows: for a dynamic PET image with n time frames, acquisition time correction factors are calculated for each 3D image voxel as the slope m of the linear regression line through n time points, multiplied by the time offset between the desired acquisition time window and the actual acquisition time window. Thus, for each voxel a corrected average value could be calculated as:

$$y_{\mathrm{CORR}} = y_{\mathrm{AVG}} + m(t_{mid\_desired} - t_{mid\_aquired}) \quad (1)$$

where $t_{mid\_desired}$ is the midpoint of the desired acquisition time window, $t_{mid\_acquired}$ is the midpoint of the actual acquisition time window, yAVG is the uncorrected mean voxel value and yCORR is the time-corrected mean voxel value.

This generates an 'image' of yCORR values which replace the original mean 20-min image and can be divided by the calculated PERSI value to produce an SUVr image (Southekal *et al.*, 2018).

Global cortical flortaucipir retention was summarized for each patient by an SUVr. The target volumes of interest (SUVr numerator) consisted of a weighted average of voxels found, through multi-block barycentric discriminant analysis (MUBADA), to contribute to discrimination between amyloid-β+ clinically defined MCI and Alzheimer's disease dementia and amyloid-β− cases at baseline. Although voxels from all brain lobes are included in this target region, the volume of interest is weighted more heavily toward voxels in posterior and lateral temporal lobe, parietal lobe and association regions of occipital cortex and exhibits higher weights in the left hemisphere (Devous *et al.*, 2018). The reference region (SUVr denominator) was parametrically derived by extracting a voxel intensity-histogram from an atlas-based white matter region, then fitting a bimodal Gaussian distribution to the histogram and using the full-width at half-maximum (FWHM) range of voxels in the lower intensity peak to construct a reference region map (PERSI reference region, Southekal *et al.*, 2018). The result is the MUBADA/PERSI flortaucipir SUVr for each subject. For supplementary analyses, SUVr were also calculated for AAL regions and a composite as previously described (Pontecorvo *et al.*, 2017*b*). Test-retest variability for various flortaucipir SUVr calculation methods has previously been examined and has been reported to be $\sim 0.0029 \pm 0.0288$ SUVr for the MUBADA/PERSI SUVr (Devous *et al.*, 2018).

Cortical surface maps were also created for each subject for the baseline, 9- and 18-month images. The baseline T_1-weighted MRI volumes were run through FreeSurfer's version 5.3 cortical reconstruction program to generate subject-specific subcortical segmentations and delineate the pial and white matter surfaces (Fischl *et al.*, 2012). The cortical reconstructions were inspected visually for failed segmentations and/or surface errors. The motion- and time-corrected baseline, 9- and 18-month flortaucipir PET scans were registered to the bias-corrected T_1 MRI generated by FreeSurfer using FSL's FLIRT function with six degrees of freedom. The flortaucipir uptake halfway between the white and pial surfaces was then projected onto Freesurfer's fsaverage template surface and smoothed by a white surface Gaussian filter with an FWHM of 5 mm. The smoothed surface maps were then normalized by each subject's PERSI reference value. Average maps were created across all amyloid-β+ subjects at baseline and 18 months and a subtraction image was used to illustrated average change in tau over 18 months. Additionally, amyloid-β+ subjects were stratified into four 'quartiles' based on their baseline MUBADA/PERSI flortaucipir SUVr values to further explore the voxel-wise change as a function of baseline flortaucipir PET signal.

All image processing and interpretation was performed blind to subject clinical status.

Statistical methods

Demographic and baseline characteristics were summarized with descriptive statistics [mean, standard deviation (SD), for continuous variables; frequency and percentages for categorical information], across all subjects, by amyloid status (florbetapir PET amyloid-β+/amyloid-β−) and by diagnosis group. Two-way ANOVA tests were performed to evaluate differences between continuous variables across amyloid status and diagnosis groups, and Mantel-Hansel χ^2 tests were applied to evaluate difference of categorical variables across amyloid status and diagnosis groups.

To evaluate the tau change at 18 months, mixed models with repeated measures (MMRM) were fitted to assess change in MUBADA SUVr while controlling for baseline MUBADA SUVr and age in amyloid-β+ and amyloid-β− groups separately, due to the concern of unequal variance in MUBADA SUVr changes observed between the amyloid-β+ and amyloid-β− groups. Similar supplementary analyses were performed using the AAL composite/cerebellum SUVr values rather than MUBADA SUVr values.

To further explore the potential factors that affect tau accumulation, a multivariate regression model with stepwise selection technique was applied. The entry and elimination criteria were set at $P = 0.20$ level due to the exploratory nature of this analysis, and the concern with this relatively small sample size. The model was run with amyloid-β+ impaired subjects (demented and MCI) only, using MUBADA SUVr change as the dependent variable. The predictors included in this model for assessment were as follows: baseline MUBADA SUVr,

florbetapir SUVr, MMSE, sex and baseline age. Similar supplementary analyses were performed using the AAL composite/cerebellum SUVr values rather than MUBADA SUVr values.

The relationship between cognitive assessments and tau level was assessed first with a simple correlation analysis. Baseline MUBADA SUVr versus MMSE change at 18 months, and change in MUBADA SUVr at 18 months versus MMSE change at 18 months were also visually displayed by scatter plots, in addition to the Pearson correlation analyses. A multivariate regression analysis with stepwise selection technique was applied to explore the contribution of each potential factor for cognitive deterioration, using amyloid-β+ impaired subjects. For this multivariate regression model, MMSE change at 18 months was used as a dependent variable, with predictors including baseline cognitive test score (i.e. MMSE), age, baseline American National Adult Reading Test (ANART; a surrogate for cognitive reserve/premorbid IQ), baseline florbetapir SUVr, APOE4 carrier status, baseline flortaucipir SUVr and/or change in flortaucipir SUVr. Entry and elimination criteria for including a predictor in the final model were set at $P = 0.20$ level. Similar analyses were also performed with ADAS and FAQ as dependent variables. Similar supplementary analyses were performed using the AAL composite/cerebellum SUVr values rather than MUBADA SUVr values.

All analyses were conducted using SAS windows version 9.4. Because of the exploratory nature of this analysis, no adjustments were made for multiplicity.

Data availability

Data that support the findings of this study are available from the corresponding author upon reasonable request.

Results

Study population baseline demographics and disposition

Table 1 shows the baseline characteristics of the 202 subjects eligible for longitudinal analysis. Supplementary Table 1 shows that the demographics for the 168 that completed the 9-month follow-up visit and the 145 that completed the 18-month visit with valid PET and cognitive data were similar to those for the baseline population. Mean age (years) increased by disease category (cognitively normal = 68.5; MCI = 70.8; clinically diagnosed Alzheimer's disease dementia = 73.9), in part because enrolment in the cognitively normal group was stratified by age to evenly cover a range from 50 to 80+ years of age. Amyloid-β+ subjects also tended to be older and more likely to be ApoE4 carriers than amyloid-β− subjects regardless of diagnostic category. The mean (SD) MMSE scores in the healthy control group were 29.5 (0.50) compared to 27.8 (1.78) in the MCI group and 21.9 (3.86) in the Alzheimer's disease dementia group. A total of 79 subjects that were classified as MCI or Alzheimer's disease dementia were amyloid-β+ and 66 subjects were amyloid-β−; in the cognitively normal group five subjects were amyloid-β+ and 52 were amyloid-β−. Dementia/MCI subjects tended to prematurely dropout of the study at a higher rate than control subjects (51/145, 35% versus 4/57, 7%, $P < 0.0001$) but there was no significant difference in the dropout rate between amyloid-β+ and amyloid-β− subjects (28/84, 33% and 28/119, 23%, respectively, $P = 0.1000$).

Table 1 Demographics for all patients receiving flortaucipir PET

	Baseline population		
	Total	Amyloid-β+	Amyloid-β−
n	202	84	118
Cognitively normal			
n	57	5	52
Age, mean years (SD)	68.5 (10.38)	77.8 (7.01)	67.6 (10.25)
Gender: female, *n* (%)	26 (45.6)	2 (40.0)	24 (46.2)
Race: Caucasian, *n* (%)	46 (80.7)	5 (100)	41 (78.8)
Education, years (SD)	15.7 (1.94)	15.2 (2.28)	15.7 (1.92)
% *APOE* 4 carriers, *n* (%)	12 (21.1)	2 (40)	10 (19.2)
MMSE mean (SD)	29.5 (0.5)	29.6 (0.55)	29.5 (0.5)
MCI			
n	97	47	50
Age, mean years (SD)	70.8 (9.35)	72.7 (9.14)	69.1 (9.29)
Gender: female, *n* (%)	48 (49.5)	21 (44.7)	27 (54.0)
Race: Caucasian, *n* (%)	88 (90.7)	45 (95.7)	43 (86.0)
Education, years (SD)	15.8 (2.95)	16.1 (2.7)	15.5 (3.17)
% *APOE* 4 carriers, *n* (%)	46 (47.4)	28 (59.6)	18 (36)
MMSE mean (SD)	27.8 (1.78)	27.4 (1.83)	28.2 (1.66)
Alzheimer's disease			
n	48	32	16
Age, mean years (SD)	73.9 (9.17)	74.8 (10.1)	72.2 (6.93)
Gender: female, *n* (%)	28 (58.3)	21 (65.6)	7 (43.8)
Race: Caucasian, *n* (%)	45 (93.8)	31 (96.9)	14 (87.5)
Education, years (SD)	15.2 (2.43)	15 (2.78)	15.6 (1.5)
% *APOE* 4 carriers, *n* (%)	26 (54.2)	22 (68.8)	4 (25)
MMSE, mean (SD)	21.9 (3.86)	21.5 (4.1)	22.9 (3.24)

Change in flortaucipir SUVr

Figure 1 shows the flortaucipir SUVr values at the three study time points (baseline, 9 and 18 months) for individual subjects as a function of their age, diagnosis and amyloid status. Consistent with our previous analysis using an AAL-derived cortical composite target area and a cerebellar crus reference region (Pontecorvo *et al.*, 2017*b*), Table 2 shows that the baseline flortaucipir SUVr [mean (standard error, SE)] was significantly higher in the amyloid-β+ subjects compared to amyloid-β− subjects [1.3267 (0.0408) versus 1.0095 (0.0034), between-group difference $P < 0.0001$]. In the amyloid-β+ group the flortaucipir SUVr [least squares mean (SE)] increased significantly from baseline to the 9- and 18-month visits [amyloid-β+:

9-month = 0.0316 (0.0060), 18-month = 0.0524 (0.0085); both $P < 0.0001$]. In the amyloid-β− group the flortaucipir SUVr was relatively unchanged with a least squares mean change in flortaucipir SUVr of −0.0003 (0.0020) and 0.0007 (0.0024) at the 9- and 18-month follow-up visits, respectively ($P > 0.78$). As has been reported previously (Pontecorvo *et al.*, 2017*b*), Fig. 1 also shows that, for the amyloid-β+ group, baseline SUVr was inversely related to age (r = −0.57, $P \leqslant 0.0001$). Figure 2A shows that there was a significant relationship between baseline flortaucipir SUVr and change in SUVr across all subjects and within the amyloid-β+ subjects only. There was also a trend in amyloid-β+ subjects toward an inverse relationship between SUVr increase and age (Fig. 2B). However, when age, sex, baseline MUBADA SUVr and florbetapir SUVr were entered as covariates, only baseline flortaucipir SUVr emerged as a significant predictor of change from baseline SUVr in the amyloid-β+ subjects. (Table 3; $P = 0.001$). Similar results (Supplementary Tables 2 and 3) were obtained using the previous (Pontecorvo *et al.*, 2017*b*) AAL composite target and cerebellar crus reference region.

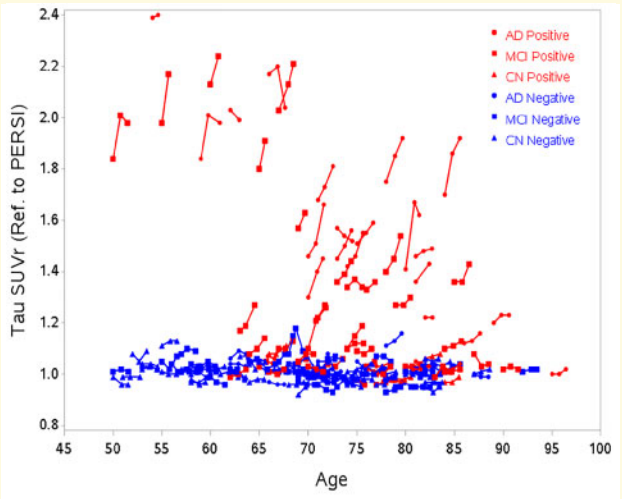

Figure 1 Flortaucipir PET MUBADA/PERSI SUVr at baseline, 9 and 18 months for individual subjects. Each subject is plotted by age at baseline and follow-up time points on the *x*-axis. Symbols reflect clinical diagnosis [cognitively normal (CN), MCI, Alzheimer's disease (AD)]. Subjects shown in red were amyloid-β+ and subjects in blue amyloid-β− by florbetapir amyloid PET scan. For amyloid-β+ subjects baseline SUVr was inversely related to age ($r = -0.57$, $P \leqslant 0.0001$).

Surface map qualitative data: all patients

Figure 3 shows Freesurfer voxel-wise surface maps of mean flortaucipir SUVr values for amyloid-β+ subjects at baseline, and the mean voxel-wise change from baseline to 18 months. Because the analysis above (Fig. 2A) suggested that baseline flortaucipir was a key determinant of SUVr change, we stratified amyloid-β+ subjects into four 'quartiles' based on their baseline MUBADA SUVr values to explore possible differences in the average pattern of voxel-wise change with increasing baseline tau load. Figure 3 suggests that the group with the lowest flortaucipir SUVr at baseline (first quartile) showed little change in SUVr over 18 months. In the group with low flortaucipir SUVr (second quartile), 18-month increases in flortaucipir were seen predominantly in inferior and lateral temporal cortex and in posterior cingulate. In subjects with intermediate flortaucipir retention at baseline (third quartile) the areas of greatest average accumulation over 18 months included posterior lateral temporal cortex, lateral occipital cortex and medial and lateral parietal cortex. Finally, in subjects with the highest levels of flortaucipir SUVr at baseline (fourth quartile), areas of greatest accumulation over 18 months included medial parietal cortex and frontal cortex. Interestingly, areas such as lateral temporal and parietal cortex, which showed the greatest degree of change in the intermediate baseline flortaucipir SUVr group (third quartile), may have begun to plateau in the highest baseline SUVr group and did not show marked increases in signal over the 18-month study period. Surface maps showing *P*-values for voxel change from baseline yielded similar conclusions (Supplementary Fig. 3).

Relationship to cognitive change

Figure 4A shows there was a moderate, but significant ($P < 0.0001$), relationship between change in MUBADA SUVr and change in MMSE that was driven by the amyloid-β+ subjects (*r* in amyloid-β+ subjects = −0.55). Figure

Table 2 Change from baseline flortaucipir MUBADA SUVr

Amyloid-β status	Baseline SUVr (±SE)	Visit	*n*	Mean change SUVr (±SE)	Mean % CFB SUVr	Least squares mean change SUVr (±SE)	*P*-value
Amyloid-β−	1.0095 (0.0034)[a]	9 months	102	−0.0003 (0.0019)	0	−0.0003 (0.0020)	0.8937
		18 months	90	0.0006 (0.0025)	0	0.0007 (0.0024)	0.7850
Amyloid-β+	1.3267 (0.0408)	9 months	66	0.0339 (0.0070)	2.2	0.0316 (0.0060)	<0.0001
		18 months	55	0.0526 (0.0095)	3.8	0.0524 (0.0085)	<0.0001

CFB = change from baseline; SE = standard error.
[a]Different from amyloid-β+, $P < 0.0001$.

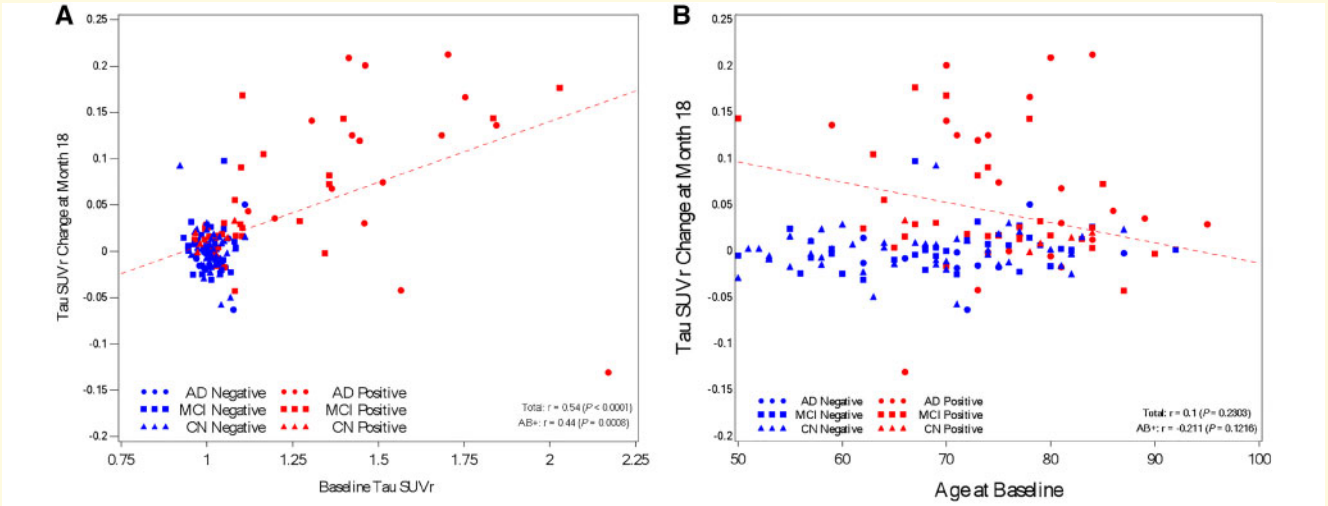

Figure 2 Correlation of baseline flortaucipir PET MUBADA SUVr (A) or age at baseline (B) with change from baseline flortaucipir PET MUBADA SUVr. Individual subjects are shown with symbols reflecting clinical diagnosis [cognitively normal (CN), MCI, Alzheimer's disease (AD)]. Subjects shown in red were amyloid-β+ and subjects in blue amyloid-β− by florbetapir amyloid PET scan. Regression line is for amyloid-β+ subjects.

Table 3 Multivariate regression model of MUBADA SUVr change at 18 months with stepwise selection technique

Fixed effect	Estimate ± SE	R-squared[a]	*P*-value[b]
Selected model			
Baseline MMSE	0.005 ± 0.0025	0.034	0.0691
Florbetapir SUVr	0.097 ± 0.0564	0.048	0.0931
Baseline MUBADA SUVr	0.117 ± 0.0334	0.174	0.0010
Overall R-squared		0.255	
Excluded effects			
Sex			0.5930
Age			0.8698

[a]Correlations for model effects are partial R-squared coefficients. Overall R-squared value is the result of the selected model.
[b]*P*-values are results from an ANCOVA analysis adjusted for the reported covariates. SE = standard error.

4A suggests that although change in flortaucipir SUVr explains a relatively modest portion (~30%) of the variance in 18-month cognitive change, there may be a threshold effect, in that all but one of the amyloid-β+ subjects with at least a 0.06 unit SUVr change showed a decline in MMSE from baseline. Because analyses suggested a strong relationship between change in SUVr and baseline SUVr (Fig. 2A), the relationship between baseline SUVr and change in cognition was also evaluated. Figure 4B indicates there was also a correlation between baseline SUVr and MMSE change from baseline (r in amyloid-β+ subjects = −0.54, $P < 0.0001$). A multivariate regression analysis with stepwise selection method was attempted to evaluate the relative contribution of baseline versus change in flortaucipir SUVr to predict change in cognition in amyloid-β+ subjects, in the context of other explanatory factors (e.g. age, APOE4 carrier status, baseline ANART, baseline florbetapir SUVr). However, sensitivity analyses indicated that the resultant model was unstable, possibly due to the limited sample size and the high degree of correlation between baseline SUVr and change in SUVr (~0.44 in amyloid-β+ subjects, 0.54 across all subjects); changes in value for just a few cases were sufficient to change the significance of baseline versus change in MUBADA SUVr as predictive factors. On the other hand, when change in SUVr was excluded from the model, baseline flortaucipir SUVr remained a significant predictor of all three measures of cognitive change (MMSE, ADAS, FAQ) even after correction for baseline test score, age, ANART and florbetapir SUVr (Table 4). Importantly, florbetapir SUVr did not survive for inclusion in any of the models when flortaucipir baseline SUVr was included. Similar results (Supplementary Table 4) were obtained using the previous (Pontecorvo *et al.*, 2017*b*) AAL composite target and cerebellar crus reference region.

Discussion

In this multicentre longitudinal evaluation of tau change using flortaucipir PET imaging, we observed a statistically significant increase in the global estimate of cortical tau burden (flortaucipir SUVr) over 18 months. This increase was amyloid-dependent, correlated with baseline flortaucipir SUVr/tau burden, and was less pronounced in older compared to younger amyloid-positive subjects. Voxel-wise evaluations further suggested that the brain regions exhibiting the greatest changes in flortaucipir PET SUVr over the 18-month study period also varied as a function

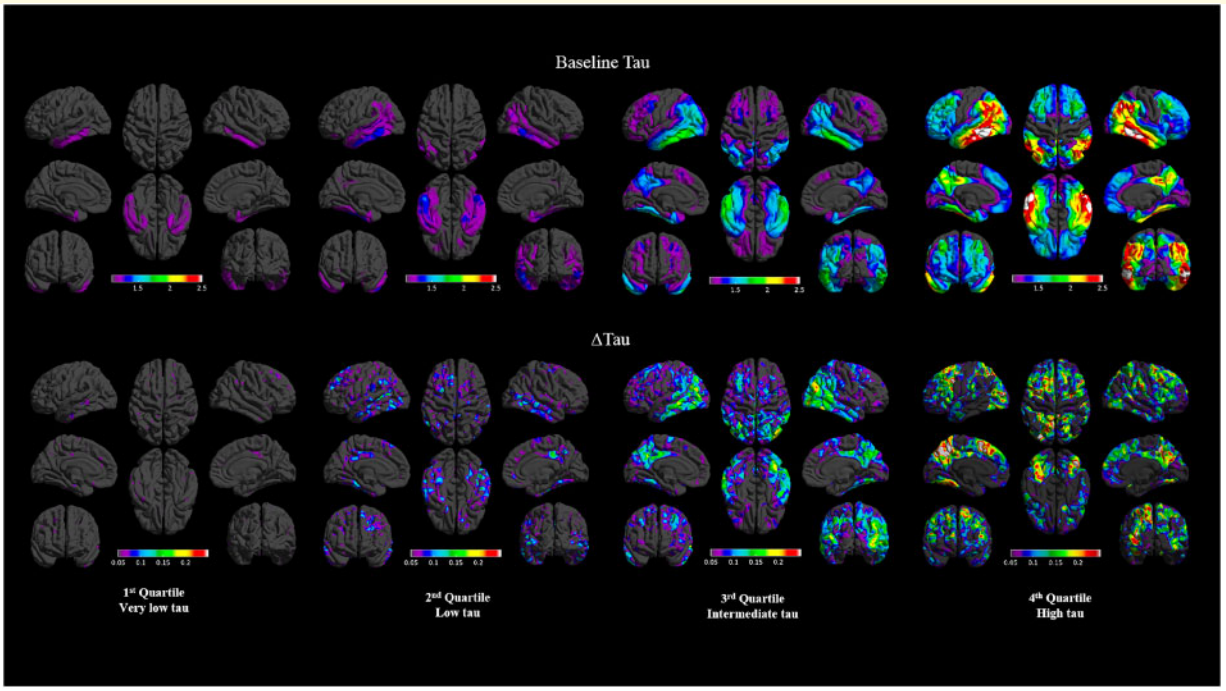

Figure 3 Freesurfer voxel-wise surface maps of mean flortaucipir SUVr values. For amyloid-β+ subjects at baseline (*top*), and the mean voxel-wise change from baseline to 18 months (*bottom*). Subjects were stratified into four 'quartiles' (*columns*) based on their baseline MUBADA SUVr values to better evaluate change in flortaucipir PET distribution as a function of baseline tau burden.

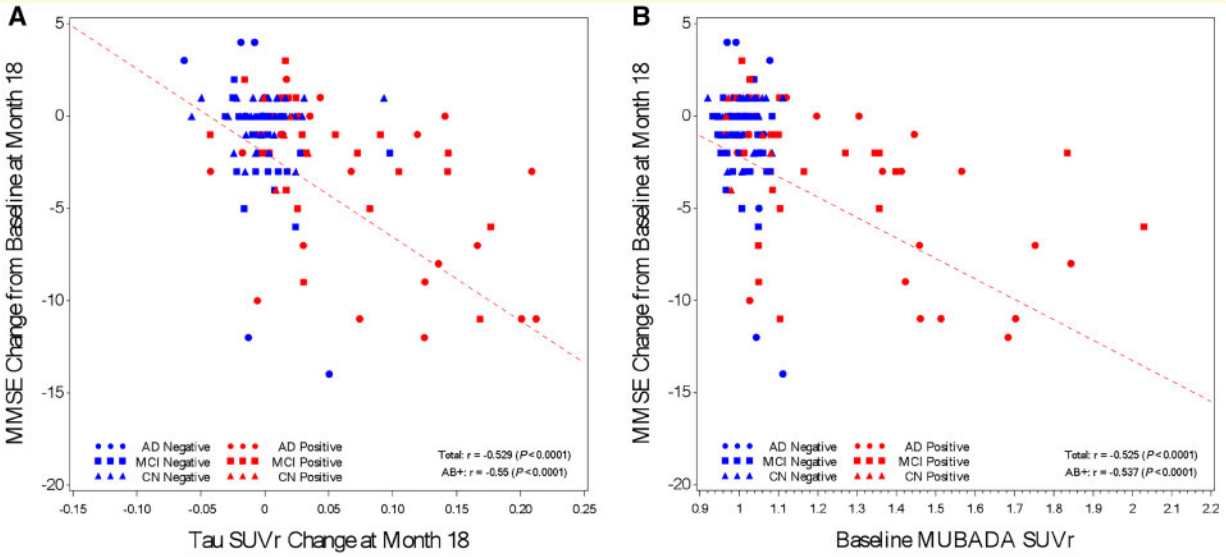

Figure 4 Correlation of change from baseline flortaucipir PET MUBADA SUVr (A) or baseline flortaucipir PET MUBADA SUVr (B) with change from baseline MMSE. Individual subjects are shown with symbols reflecting clinical diagnosis [cognitively normal (CN), MCI, Alzheimer's disease (AD)]. Subjects shown in red were amyloid-β+ and subjects in blue amyloid-β− by florbetapir amyloid PET scan. Regression line is for amyloid-β+ subjects.

of baseline global estimate of tau burden. Finally, change in flortaucipir SUVr, and perhaps more importantly, baseline flortaucipir SUVr were significantly associated with changes in cognitive performance as assessed by MMSE, ADAS and FAQ.

The absence of a measurable change in flortaucipir SUVr in amyloid-β− subjects (0.0005 SUVr units over 18 months), in contrast to the significant change in amyloid-β+ subjects, suggests that amyloid deposition may be a necessary antecedent for spread of tau beyond the temporal

Table 4 Stepwise regression: predictors of cognitive change

	Baseline MUBADA	Baseline Cog Test	Age	ANART	Florbetapir SUVr	APOE4	Model total
MMSE							
r^2	0.301	NS	NS	0.050	NS	0.043	0.395
P	0.0016	>0.2	>0.2	0.058	>0.2	0.0831	
ADAS							
r^2	0.0667	NS	0.0328	0.2136	NS	NS	0.313
P	0.0210	>0.2	0.1589	0.0087	>0.2	>0.2	
FAQ							
r^2	0.13	NS	NS	NS	NS	NS	0.130
P	0.01	>0.2	>0.2	>0.2	>0.2	>0.2	

ADAS = Alzheimer's Disease Assessment Scale 11-item cognitive subscale; FAQ = Pfeffer Functional Activities Questionnaire; NS = not significant.

lobe in Alzheimer's disease. It is worth noting that the amyloid-β− group in this study (in contrast to the recent study of Jack *et al.*, 2018) contained a significant number of cognitively impaired individuals (50 clinically diagnosed MCI, 16 possible/probable Alzheimer's disease dementia at baseline) so the pattern of cross-sectional and longitudinal change in flortaucipir PET signal observed in the amyloid-β+ group cannot simply be attributed to the presence of impairment, but is likely associated with Alzheimer's disease pathology. Emerging evidence indicates that the sensitivity of flortaucipir and the regional pattern of flortaucipir retention may be different in non-Alzheimer's disease tauopathies than in Alzheimer's disease (Josephs *et al.*, 2016; McMillan *et al.*, 2016; Ossenkoppele *et al.*, 2016; Smith *et al.*, 2016; Hammes *et al.*, 2017; Marquié, 2017; Schonhaut *et al.*, 2017), and may even differ between Alzheimer's disease and associated dementias such as dementia with Lewy bodies (Gomperts *et al.*, 2016; Kantarci *et al.*, 2017). Thus, it remains to be determined whether the rates of longitudinal change observed in this study have any generalizability to non-Alzheimer's disease tauopathies.

Examination of individual changes in tau in Fig. 1, or the least squares mean change values at 9 and 18 months in Table 2, suggests that the change in global cortical tau is roughly linear for individual subjects over the 18-month period (e.g. the change over the first 9 months is comparable to change over the second 9 months). However, rate of change in tau accumulation might not be linear over the longer course of the disease. Figure 2 shows that the magnitude of change over the 18-month period varied as a function of the baseline SUVr value. Thus, it might be expected that over a longer period of time the rate of increase in the global estimate of tau might increase with disease severity. These results are consistent with the hypothesis of trans-synaptic spread of tau (De Calignon *et al.*, 2012; Liu *et al.*, 2012), in that it would be expected that the higher the baseline SUVr, the greater the number of neurons affected. This, in turn, would lead to a greater number of at risk synapses and thus, a greater degree of increase in tau over the observation period.

Voxel-wise analysis provided further evidence of a different rate and pattern of tau change as a function of flortaucipir global SUVr at baseline. In subjects with low or no elevation of flortaucipir retention at baseline, the greatest changes in SUVr were seen in inferior and lateral temporal cortex and in posterior cingulate. With increasing baseline tau burden, more posterior brain regions (e.g. occipital and parietal cortex) seemed to become important, whereas in subjects with the highest levels of flortaucipir SUVr at baseline, the areas of greatest accumulation also included frontal cortex. However, in subjects with the highest levels of flortaucipir SUVr at baseline, some regions such as lateral temporal and parietal cortex did not change substantially, suggesting that the tau pathology in these areas may have reached a plateau. This pattern of changes is consistent with cross-sectional descriptions of tau staging and provides preliminary longitudinal evidence that tau spread, at least at a group level, may follow the pattern predicted from cross-sectional autopsy studies. The results also provide some measure of caution regarding use of global measures of tau change as outcomes in longitudinal studies, since different regions may be changing at different rates over time depending on the severity and location of the initial/baseline tau burden.

A possible weakness of this study is that the proportion of amyloid-β− Alzheimer's disease dementia patients is higher (33%) than in some previous studies. This may be due in part to the use of a possible, rather than a probable Alzheimer's disease diagnosis as an entry criterion in the present study. For example, a 22% amyloid-β− rate was reported in a therapeutic trial of probable Alzheimer's disease subjects (Siemers *et al.*, 2016) whereas a recent study in patients seeking diagnosis reported that ∼30% of subjects with possible Alzheimer's disease as a working diagnosis prior to scan were amyloid-β− by florbetapir read (Pontecorvo *et al.*, 2017*c*). Although the amyloid-β− subjects reduce the power to examine changes in the population of interest (amyloid-β+/Alzheimer's disease pathology subjects), the amyloid-β− cohort does, as noted above, provide an interesting population to compare tau changes (or lack of changes) in the absence of amyloid. A potentially

more important weakness is the low number of amyloid-β+ clinically normal subjects in this study. This makes it difficult to evaluate tau/flortaucipir retention at the earliest stages of the Alzheimer's continuum.

Another weakness of this study is that the effects of age and baseline SUVr in this study were largely confounded. The younger subjects tended to have the highest baseline SUVr, and young age was also associated with increased change in SUVr from baseline to 18 months. The elevated baseline SUVr and more rapid increase in SUVr in the younger subjects over the 18-month study period may indicate a more aggressive Alzheimer's disease pathology in patients with younger age at onset. However, this finding may also reflect a survivor effect in the older subjects. Moreover, factors other than Alzheimer's disease pathology are increasingly likely to contribute to cognitive impairment as individuals age (Jack *et al.*, 2016). As a result of the additive effects of other neuropathology plus tau burden/Alzheimer's disease pathology, older subjects may have greater impairment than young subjects at any given level of pathology, and older subjects with the highest levels of tau burden/Alzheimer's disease pathology, comparable to that seen in the young subjects, might be too impaired to participate in a study of this type. The complicated relationship between age, tau burden and cognitive impairment has previously been reported both in tau PET studies (Cho *et al.*, 2017; Pontecorvo *et al.*, 2017*b*; Schöll *et al.*, 2017) and clinicopathological studies (Prohovnik *et al*, 2006; Middleton *et al*, 2011).

Overall the results of this study are similar in many respects to the longitudinal changes in tau accumulation recently reported by Jack *et al.* (2018). In both studies, amyloid-β+ cognitively impaired subjects showed longitudinal accumulation of cortical flortaucipir signal (presumed accumulation of tau) whereas amyloid-β− subjects did not. The magnitude of effect (about 2–3% per year relative to baseline SUVr) was remarkably similar despite the differences in method for SUVr calculation, duration of follow-up and differences in the subject populations (a longitudinal community sample versus a clinical trial sample). Both studies also reported an inverse relationship between age and baseline SUVr and a trend for younger subjects with higher baseline SUVr to also show greater longitudinal change.

However, this study also extends the Jack *et al.* (2018) study in two important ways. First, by stratifying the subjects into 'quartiles' on the basis of baseline SUVr values and evaluating change at a voxel level, we were able to see quartile-related (presumably disease severity-related) differences in focal flortaucipir accumulation that were probably averaged out in the Jack *et al.* (2018) analysis. Second, we not only examined the longitudinal change in flortaucipir PET signal, but we evaluated the relationship association of baseline flortaucipir SUVr, and change in flortaucipir SUVr with cognitive deterioration.

Both baseline and change from baseline in flortaucipir global (MUBADA/PERSI) SUVr were associated with decrease in cognitive performance in amyloid-β+ subjects, even after correction for age, cognitive reserve (ANART), APOE4 carrier status and amyloid burden (florbetapir PET SUVr). Importantly, florbetapir SUVr was not retained in any of the models as a predictor of cognitive change as assessed by MMSE, ADAS or FAQ, consistent with the hypothesis that amyloid burden enables the spread of tau, but tau, rather than amyloid, is proximally related to neuronal dysfunction and associated cognitive impairment in Alzheimer's disease (Nelson *et al.*, 2007; Jack *et al.*, 2016; Pontecorvo *et al.*, 2017*b*).

Change in flortaucipir SUVr was strongly correlated with baseline flortaucipir SUVr, but the sample size was too small to confidently perform analyses to separate the effects of baseline and change in flortaucipir SUVr on cognitive performance. Baseline flortaucipir SUVr presumably represents the cumulative brain exposure to tau NFT at the time of the baseline scan, and will reflect both the neuronal damage that has accumulated during the course of the disease, as well as the regions where ongoing neurodegeneration is likely to impact cognition in the future. In contrast, change in flortaucipir SUVr reflects only spread of tau within the 18-month observation period, and some portion of this recently accumulated tau may not yet have had a significant impact on neuronal function. Additional studies (e.g. the ongoing confirmatory arm of the present study, NCT# 02016560) and a larger sample size are needed to determine the relative contributions of these factors. Such studies could help confirm whether there may be some delay between appearance of tau tangles and expression of neuronal damage in the form of cognitive deterioration as predicted by recent models of the progression of Alzheimer's disease (Jack *et al.*, 2013).

Taken together, these results provide longitudinal evidence that tau spread may follow the pattern predicted from cross-sectional autopsy studies. Moreover, these results suggest that the amount and location of tau (as evidenced by flortaucipir SUVr) at baseline may have implications both for the spread of tau and the cognitive deterioration that may occur over an 18-month period. These results suggest that it may be possible, even necessary, to use baseline tau as a selection or stratifying variable in clinical trials, instead of, or in addition to, currently used variables such as neuropsychological tests and amyloid status, thus reducing the expected variance in disease progression and cognitive change and improving the power to detect a therapeutic effect.

Funding

This study was sponsored and funded by Avid Radiopharmaceuticals a wholly owned subsidiary of Eli Lilly and Company.

Competing interests

M.J.P., M.D.D. Sr, M.N., M.L., N.G., A.K.A., S.S., A.M., N.C.L., H.X., S.P.T., A.D.J., S.S., B.T, A.S.F. and M.A.M. are employees of Eli Lilly and Company and/or Avid Radiopharmaceuticals, and are minor shareholders of Eli Lilly and Company. S. Salloway receives research support and consultancy fees from Lilly, Biogen, Merck, Genentech, and Roche. He also receives research support from Avid, Novartis, and Functional Neuromodulation. P.M.D. received a grant (through his university) from Avid Radiopharmaceuticals and has received grants from and/or served as an advisor to several companies in this field. He is also a minor shareholder in several companies whose products are not discsused here and a co-inventor on patents which are not discussed here.

Supplementary material

Supplementary material is available at *Brain* online.

References

Albert, M. S., DeKosky, S. T., Dickson, D., Dubois B, Feldman HF, Fox NC, et al. The diagnosis of mild cognitive impairment due to Alzheimer's disease: recommendations from the National Institute on Aging and Alzheimer's Association workgroup. Alzheimer's Dement, 2011; 7: 270–9.

Baker, JE, Lim YY, Pietrzak RH, Hassenstab J, Snyder PJ, Masters C, et al. Cognitive impairment and decline in cognitively normal older adults with high amyloid-β: A meta analysis. Alzheimer's Dement 2017; 6: 108–21.

Bennett DA, Schneider JA, Bienias JL, Evans DA, Wilson RS. Mild cognitive impairment is related to Alzheimer's disease pathology and cerebral infarctions. Neurology 2005; 64: 834–41.

Berg L, McKeel DW Jr, Miller P, Storandt M, Rubin EH, Morris JC, et al. Clinicopathologic studies in cognitively healthy aging and Alzheimer disease. Arch Neurol 1998; 55: 326–35.

Betthauser TJ, Cody KA, Zammit MD, Murali D, Converse AK, Barnhart TE, et al. In vivo characterization and quantification of neurofibrillary tau PET radioligand MK-6240 in humans from Alzheimer's disease dementia to young controls. J Nucl Med 2019; 60: 93–99.

Bouras C, Hof PR, Giannakopoulos Pl, Michel JP, Morrison JH. Regional distribution of neurofibrillary tangles and senile plaques in the cerebral cortex of elderly patients: a quantitative evaluation of a one-year autopsy population from a geriatric hospital. Cerebral Cortex 1994; 4: 138–50.

Braak H, Alafuzoff I, Arzberger T, Kretzschmar H, Del Tredici K. Staging of Alzheimer disease-associated neurofibrillary pathology using paraffin sections and immunocytochemistry. Acta Neuropathol 2006; 112: 389–404.

Brier MR, Gordon B, Friedrichsen K, McCarthy J, Stern A, Christensen J, et al. Tau and Aβ imaging, CSR measures, and cognition in Alzheimer's disease. Sci Transl Med 2016; 8: 338ra66.

Chien DT, Szardenings AK, Bahri S, Walsh JC, Mu F, Xia C, et al. Early Clinical PET imaging results with the novel PHF-tau radioligand [F18]-T808. J Alzheimers Dis 2014; 38: 171–84.

Cho H, Choi JY, Hwang MS, Kim YJ, Lee HM, Lee HS, et al. In vivo cortical spreading patter of tau and amyloid in the Alzheimer's disease spectrum. Ann Neurol 2016a; 80: 247–58.

Cho H, Choi JY, Hwang MS, Lee JH, Kim YJ, Lyoo CH, et al. Tau PET in Alzheimer disease and mild cognitive impairment. Neurology 2016b; 87: 375–83.

Cho H, Choi JY, Lee SH, Lee JH, Choi YC, Ryu YH, et al. Excessive tau accumulation in the parieto-occipital cortex characterizes early-onset Alzheimer's disease. Neurobiol Aging. 2017; 53: 103–11.

Clark CM, Pontecorvo MJ, Beach TG, Bedell BJ, Coleman RE, Doraiswamy PM, et al. Cerebral PET with florbetapir compared with neuropathology at autopsy for detection of neuritic amyloid-beta plaques: a prospective cohort study. Lancet Neurol 2012; 11: 669–78.

Crary JF, Trojanowski JQ, Schneider JA, Abisambra JF, Abner EL, Alafuzoff I, et al. Primary age-related tauopathy (PART): a common pathology associated with human aging. Acta Neuropathol 2014; 128: 755–66.

Cummings BJ, Pike CJ, Shankle R, Cotman CW. Beta-amyloid deposition and other measures of neuropathology predict cognitive status in Alzheimer's disease. Neurobiol Aging 1996; 17: 921–33.

Curtis C, Gamez JE, Singh U, Sadowsky CH, Villena T, Sabbagh MN, et al. Phase 3 trial of flutemetamol labeled with radioactive fluorine 18 imaging and neuritic plaque density. JAMA Neurology 2015; 72: 287–94.

De Calignon A, Polydoro M, Suarez-Calvet M, William C, Adamowicz DH, Kopeikina KJ, et al. Propogation of tau pathology in a model of early Alzheimer's disease. Neuron 2012; 73: 685–97.

Declercq L, Rombouts F, Koole M, Fierens K, Mariën J, Langlois X, et al. Preclinical evaluation of ^{18}F-JNJ64349311, a novel PET tracer for tau imaging. J Nucl Med. 2017; 58: 975–81.

Devous MD Sr, Joshi AD, Navitsky M, Southekal S, Pontecorvo MJ, Siderowf A, et al. Test-retest reproducibility for the tau PET imaging agent flortaucipir F18. J Nucl Med 2018; 59: 937–43.

Doraiswamy PM, Sperling RA, Coleman RE, Johnson KA, Reiman PEM, Davis MD, et al. Florbetapir F 18 amyloid PET and longitudinal cognitive decline: a prospective 36-month multicenter study. Mol Psychiatry 2014; 19: 1044–51.

Fischl, B. FreeSurfer. Neuroimage 2012; 62: 774–81.

Fonov V, Evans AC, Botteron K, Almli CR, McKinstry RC, Collins DL et al. Unbiased average age-appropriate atlases for pediatric studies. NeuroImage 2011; 54: 313–27.

Friston KJ, Ashburner JT, Kiebel SJ, Nichols TE, Penny WD, editors. Statistical Parametric Mapping: The Analysis of Functional Brain Images. London: Academic Press; 2007.

Gomperts SN, Locascio JJ, Makaretz SJ, Schultz A, Caso C, Vasdev N, et al. Tau positron emission tomographic imaging in the lewy body diseases. JAMA Neurol. 2016; 73: 1334–41.

Hammes J, Bischof GN, Giehl K, Faber J, Drzezga A, Klockgether T, et al. Elevated in vivo [18F]-AV-1451 uptake in a patient with progressive supranuclear palsy. Mov Disord 2017; 32: 170–1.

Harada R, Okamura N, Furumoto S, Furukawa K, Ishiki A, Tomita N, et al. ^{18}F-THK5351: a novel PET radiotracer for imaging neurofibrillary pathology in Alzheimer disease. J Nucl Med 2016; 57: 208–14.

Hostetler ED, Walji AM, Zeng Z, Miller P, Bennacef I, Salinas C, et al. Preclinical Characterization of 18F-MK-6240, a promising PET tracer for in vivo quantification of human neurofibrillary tangles. J Nucl Med 2016; 57: 1599–606.

Hulette CM[1], Welsh-Bohmer KA, Murray MG, Saunders AM, Mash DC, McIntyre LM. Neuropathological and neuropsychological changes in "normal" aging: evidence for preclinical Alzheimer disease in cognitively normal individuals. J Neuropathol Exp Neurol 1998; 57: 1168–74.

Hyman BT, Phelps CH, Beach TG, Bigio EH, Cairns NJ, Carrillo MC, et al. National Institute on Aging Alzheimer's Association guidelines for the neuropathologic assessment of Alzheimer's disease. Alzheimers Dement 2012; 8: 1–13.

Jack CR, Knopman DS, Jagust WJ, Petersen RC, Weiner MW, Aisen PS, et al. Tracking pathophysiological processes in Alzheimer's

disease: an updated hypothetical model of dynamic biomarkers. Lancet Neurol 2013; 12: 207–16.

Jack CR, Therneau TM, Wiste HJ, Weigand SD, Knopman DS, Lowe VJ, et al. Transition rates between amyloid and neurodegeneration biomarker states and to dementia: a population-based longitudinal cohort study. Lancet Neurol 2016; 15: 56–64.

Jack, CR, Wiste HJ, Schwarz CG, Lowe VJ, Senjem ML, Vemuri P, et al. Longitudinal tau PET in aging and Alzheimer's disease. Brain 2018; 141: 1517–28.

Johnson, K.A., Sperling, R.A., Gidicsin, C., Carmasin, J., Maye, J., Coleman, et al. Florbetapir (F18-AV-45) PET to assess amyloid burden in Alzheimer's disease dementia, mild cognitive impairment, and normal aging. Alzheimer's Dement 2013; 9: S72–83.

Johnson KA, Schultz A, Betensky RA, Becker JA, Sepulcre J, Rentz D, et al. Tau positron emission tomographic imaging in aging and early Alzheimer disease. Ann Neurol 2016; 79: 110–19.

Josephs KA, Whitwell JL, Tacik P, Duffy JR, Senjem ML, Tosakulwong N, et al. [18F]AV-1451 tau-PET uptake does correlate with quantitatively measured 4R-tau burden in autopsy-confirmed corticobasal degeneration. Acta Neuropathol 2016; 132: 931–3.

Kantarci K, Lowe VJ, Boeve BF, Senjem ML, Tosakulwong N, Lesnick TG, et al. AV-1451 tau and β-amyloid positron emission tomography imaging in dementia with Lewy bodies. Ann Neurol 2017; 81: 58–67.

Knopman DS, Parisi JE, Salviati A, Floriach-Robert M, Boeve BF, Ivnik RJ, et al. Neuropathology of cognitively normal elderly. J Neuropathol Exp Neurol 2003; 62: 1087–95.

Liu L, Drouet V, Wu J, Witter MP, Small SA, Clelland C, et al. Trans-synaptic spread of tau pathology in vivo. PLoS One 2012; 7: e31302.

Lockhart SN, Baker SL, Okamura N, Furukawa K, Ishiki A, Furumoto S, et al. Dynamic PET Measures of Tau Accumulation in Cognitively Normal Older Adults and Alzheimer's Disease Patients Measured Using [18F] THK-5351. PLoS One 2016; 11: e0158460.

Ma Y, Zhang S, Li J, Zheng DM, Guo Y, Feng J, et al. Predictive accuracy of amyloid imaging for progression from mild cognitive impairment to Alzheimer disease with different lengths of follow-up: a meta-analysis. Medicine 2014; 93: e150.

Marquié M, Normandin MD, Meltzer AC, Chong MST, Andrea NV, Antón-Fernández A, et al. Pathologic correlations of [F-18]-AV-1451 imaging in non-Alzheimer tauopathies. Ann Neurol 2017; 81: 117–28.

Maruyama M, Shimada H, Suhara T, Shinotoh H, Ji B, Maeda J, et al. Imaging of tau pathology in a tauopathy mouse model and in Alzheimer patients compared to normal controls. Neuron 2013; 79: 1094–108.

McKhann, G.M., Knopman, D.S., Chertkow, H., Hyman BT, Jack CR, Kawas CH, et al. The diagnosis of dementia due to Alzheimer's disease: recommendations from the National Institute on Aging-Alzheimer's Association workgroups on diagnostic guidelines for Alzheimer's disease. Alzheimers Dement 2011; 7: 263–69.

McMillan, C. T., Irwin, D. J., Nasrallah, I., Phillips, J. S., Spindler, M., Rascovsky, K., et al. Multimodal evaluation demonstrates *in vivo* ^{18}F-AV-1451 uptake in autopsy-confirmed corticobasal degeneration. Acta Neuropathol 2016; 132: 935–7.

Middleton LE, Grinberg LT, Miller B, Kawas C, Yaffe K. Neuropathologic features associated with Alzheimer disease diagnosis: age matters. Neurology 2011; 77: 1737–44.

Mungas D, Tractenberg R, Schneider JA, Crane PK, Bennett DA. A two-process model for neuropathology of Alzheimer's disease. Neurobiology of Aging 2014; 35: 301–8.

Nelson PT, Jicha GA, Schmitt FA, Liu H, Davis DG, Mendiondo MS, et al. Clinicopathologic correlations in a large Alzheimer disease center autopsy cohort: neuritic plaques and neurofibrillary tangles "do count" when staging disease severity. J Neuropathol Exp Neurol 2007; 66: 1136–46.

Nelson PT, Braak H, Markesbery WR. Neuropathology and cognitive impairment in Alzheimer disease: a complex but coherent relationship. J Neuropath Exp Neurol 2009; 68: 1–14.

Nelson PT, Alafuzoff I, Bigio EH, Bouras C, Braak H, Cairns NJ, et al. Correlation of Alzheimer disease neuropathologic changes with cognitive status: a review of the literature. J Neuropathol Exp Neurol 2012; 71: 362–81.

Okamura N, Furumoto S, Fodero-Tavoletti MT, Mulligan RS, Harada R, Yates P, et al. Non-invasive assessment of Alzheimer's disease neurofibrillary pathology using 18F-THK5105 PET. Brain 2014; 137: 1762–71.

Ossenkoppele R, Schonhaut DR, Scholl M, Lockhart SN, Ayakta N, Baker SL, et al. Tau PET patterns mirror clinical and neuroanatomical variability in Alzheimer's disease. Brain 2016; 139: 1551–67.

Pike KE, Savage G, Villemagne VL, Ng S, Moss SA, Maruff P, et al. β-amyloid imaging and memory in non-demeted individuals: evidence for preclinical Alzheimer's disease. Brain 2007; 130: 2837–44.

Pontecorvo MJ, Arora AK, Devine M, Lu M, Galante N, Siderowf A, et al. Quantitation of PET signal as an adjunct to visual interpretation of florbetapir imaging. E J Nuc Med 2017a; 44: 825–37.

Pontecorvo MJ, Devous MD Sr, Navitsky M, Lu M, Salloway S, Schaerf FW, et al. Relationships between flortaucipir (^{18}F-AV-1451) positron emission tomography tau binding and amyloid burden clinical diagnosis, age and cognition. Brain 2017b; 140: 748–63.

Pontecorvo MJ, Siderowf A, Dubois B, Doraiswamy PM, Frisoni GB, Grundman M, et al. Effectiveness of florbetapir PET imaging in changing patient management. Dement Geriatr Cogn Disord 2017c; 44: 129–43.

Price JL, Morris JC. Tangles and plaques in nondemented aging and "preclinical" Alzheimer's disease. Ann Meurol 1999; 45: 358–68.

Prohovnik I, Perl DP, Davis KL, Libow L, Lesser G, Haroutunian V. Dissociation of neuropathology from severity of dementia in late-onset Alzheimer disease. Neurology 2006; 66: 49–55.

Sabri O, Sabbagh MN, Seibyl J, Barthel H, Akatsu H, Ouchi Y, et al. Florbetaben PET imaging to detect amyloid beta plaques in Alzheimer's disease: phase 3 study. Alzheimers Dement 2015; 11: 964–74.

Shcherbinin S, Schwarz AJ, Joshi AJ, Navitsky M, Flitter M, Shankle WR, et al. Kinetics of the tau PET tracer [^{18}F]-AV-1451 (T807) in subjects with normal cognitive function, mild cognitive impairment and Alzheimer's disease. J Nuc Med 2016; 10: 1535–42.

Schonhaut DR, McMillan CT, Spina S, Dickerson BC, Siderowf S, Devous MD Sr, et al. ^{18} F-flortaucipir tau positron emmission tomography distinguishes established progressive supranuclear palsy from controls and Parkinson disease: a multicenter study. Ann Neurol 2017; 82: 622–34.

Schöll M, Lockhart SN, Schonhaut DR, O'Neil JP, Janabi M, Ossenkoppele R, et al. PET imaging of Tau deposition in the aging human brain. Neuron 2016; 89: 971–82.

Schöll M, Ossenkoppele R, Strandberg O, Palmqvist S, Jögi J, et al.; Swedish BioFINDER study. Distinct 18F-AV-1451 tau PET retention patterns in early- and late-onset Alzheimer's disease. Brain 2017; 140: 2286–94.

Schwarz AJ, Yu P, Miller BB, Shcherbinin S, Dickson J, Navitsky M, et al. Regional profiles of the candidate tau PET ligand ^{18}F-AV-1451 recapitulate key features of Braak histopathological stages. Brain 2016; 139: 1539–50.

Selkoe DJ. The molecular pathology of Alzheimer's disease. Neuron 1991; 6: 487–98.

Siemers ER, Sundell KL, Carlson C, Case M, Sethuraman G, Liu-Seifert H. et al. Phase 3 solanezumab trials: secondary outcomes in mild Alzheimer's disease patients. Alzheimer's Dement 2016; 12: 110–20.

Smith R, Puschmann A, Schöll M, Ohlsson T, van Swieten J, Honer M, et al. 18F-AV-1451 tau PET imaging correlates strongly with tau neuropathology in MAPT mutation carriers. Brain 2016; 139: 2372–9.

Saint-Aubert L, Lemoine L, Chiotis K, Leuzy A, Rodriguez-Vieitez E, Nordberg A. Tau PET imaging: present and future directions. Mol Neurodegener 2017; 12: 19.

Southekal S, Devous MD Sr., Kennedy I, Navitsky M, Lu M, et al. Flortaucipir F 18 quantitation using a parametric estimate of reference signal intensity (PERSI). J Nucl Med 2018; 59: 944–951.

Tomlinson BE, Blessed G, Roth M. Observations on the brains of demented old people. J Neurol Sci 1970; 11: 205–42.

Villemagne VL, Dore V, Bourgeat P, Burnham SC, Laws S, Salvado O, et al. Aβ-amyloid and tau imaging in dementia. Semin Nucl Med 2017; 47: 75–88.

Wong DF, Comley R, Kuwabara H, Rosenberg PB, Resnick SM, Ostrowitzki S, et al. First in-human PET study of 3 novel tau radiopharmaceuticals: [^{11}C]RO6924963, [^{11}C]RO6931643, and [^{18}F]RO6958948. J Nucl Med 2018; 59: 1869–76.

World Medical Association. Declaration of Helsinki. Recommendations guiding physicians in biomedical research involving human subjects. JAMA 1997; 277: 925–6.

Xia CF, Arteaga J, Chen G, Gangadharmath U, Gomez LF, Kasi D, et al. [18F]T807, a novel tau positron emission tomography imaging agent for Alzheimer's disease. Alzheimers Dement 2013; 9: 666–76.